



Molecular Crystals and Liquid Crystals Incorporating Nonlinear Optics

Publication details, including instructions for authors and
subscription information:

<http://www.tandfonline.com/loi/gmcl17>

Optical Properties of Chiral Nematic Liquid Crystals

H. F. Gleeson^a & H. J. Coles^a

^a Liquid Crystal Group, Physics Department, The University,
Manchester, M13 9PL, United Kingdom

Version of record first published: 04 Oct 2006.

To cite this article: H. F. Gleeson & H. J. Coles (1989): Optical Properties of Chiral Nematic Liquid Crystals, *Molecular Crystals and Liquid Crystals Incorporating Nonlinear Optics*, 170:1, 9-34

To link to this article: <http://dx.doi.org/10.1080/00268948908047744>

PLEASE SCROLL DOWN FOR ARTICLE

Full terms and conditions of use: <http://www.tandfonline.com/page/terms-and-conditions>

This article may be used for research, teaching, and private study purposes. Any substantial or systematic reproduction, redistribution, reselling, loan, sub-licensing, systematic supply, or distribution in any form to anyone is expressly forbidden.

The publisher does not give any warranty express or implied or make any representation that the contents will be complete or accurate or up to date. The accuracy of any instructions, formulae, and drug doses should be independently verified with primary sources. The publisher shall not be liable for any loss, actions, claims, proceedings, demand, or costs or damages whatsoever or howsoever caused arising directly or indirectly in connection with or arising out of the use of this material.

Optical Properties of Chiral Nematic Liquid Crystals

H. F. GLEESON and H. J. COLES

Liquid Crystal Group, Physics Department, The University, Manchester, M13 9PL, United Kingdom

(Received July 5, 1988; in final form September 28, 1988)

The selective reflection of light from thermochromic liquid crystals is characterized by the peak wavelength (λ_p) and width ($\Delta\lambda$) of the reflection spectrum and may be related theoretically to the average refractive index (\bar{n}), the birefringence (Δn) and the pitch (p) of the material. We have examined the influence of each of these parameters, varied and measured independently, for two series of new chiral nematic mixtures. Materials are described with birefringences in the range $0.04 \leq \Delta n \leq 0.16$ and the equivalence of $\lambda_p/\Delta\lambda$ and $\bar{n}/\Delta n$ has been studied. We have shown that the relationship is valid for large values of Δn , but holds less well as Δn becomes small ($\Delta n \leq 0.1$). In the second series of materials, we have considered the influence of twisting power alone. In the absence of other variables (i.e., birefringence, transition temperatures, etc.), a decrease in the twisting power gave only an associated increase in the selective reflection wavelength. We conclude that changes in birefringence or twisting power alone do not alter the functional dependence of λ_p on temperature.

1. INTRODUCTION

Thermochromism in chiral nematic liquid crystals is a result of the selective reflection of light by the helical structure of the mesophase. As the pitch of the helix changes with temperature, so, too, does the peak wavelength (λ_p) of the selective reflection spectrum. For a well aligned planar film of chiral nematic liquid crystal this relatively narrow spectrum may be characterized in terms of the helical pitch p , the mean refractive index \bar{n} [$= \frac{1}{2}(n_o + n_e)$] and the birefringence Δn ($= n_o - n_e$) of the system. The interdependence of these parameters was postulated by de Vries¹ to be:

$$\lambda_p = \bar{n}p \quad (1)$$

and

$$\lambda_p/\Delta\lambda = \bar{n}/\Delta n, \quad (2)$$

where $\Delta\lambda$ describes the width of the selective reflection spectrum. In temperature sensing devices based on thermochromic liquid crystals, λ_p indicates temperature and $\Delta\lambda$ defines the resolution and brightness. Although both \bar{n} and Δn vary with

temperature, to some extent the variations are usually small and it is primarily pretransitional changes in the pitch, as a low temperature smectic phase is approached, which give the rapid color changes used in thermochromic devices.²⁻⁴ The extent of this pretransitional behavior varies greatly between materials. However, at any defined temperature, Equations (1) and (2) should always describe the spectral characteristics of the selective reflection irrespective of the chemical composition of the thermochromic material.

New stable chiral nematic materials have been synthesized by Gray et al.⁵ and Demus et al.⁶ and these have begun to replace cholesteryl esters for use in thermochromic devices. The availability⁷ of the new materials and the range of their optical properties has afforded an opportunity to examine the validity of the de Vries equations in some detail. In this paper we will examine the effects of varying independently the birefringence or the twisting power of the chiral nematic materials on the selective reflection properties. Two series of mixtures have been developed to allow the influence of these two parameters to be evaluated. In the first part of the paper we concentrate on the effects of birefringence alone. Refractive index data measured using an Abbé refractometer, with Δn varied between 0.04 and 0.16, will be used to calculate the ratio $\bar{n}/\Delta n$. This will then be compared with $\lambda_p/\Delta\lambda$, measured from the selective reflection spectra, over a wide range of temperatures. In the second part, we will consider the influence of twisting power alone. Although it is known that long pitch materials give selective reflections at long wavelengths [c.f., Equation (1)], and vice versa for short pitch materials, it is not known whether the twisting power has any influence on the form of the selective reflection as a function of temperature. A system of mixtures has been evolved in which the twisting power is the only variable, i.e., in which the phase behavior, transition temperatures and refractive indices are constant, so that its role in determining the form of the color-play may be unequivocally evaluated. The results of the two sets of experiments, i.e., varying birefringence and twisting power, will be discussed in terms of the implications for thermochromic devices.

2. MEASUREMENT OF THE SELECTIVE REFLECTION SPECTRA

For each series of chiral nematic materials it was necessary to measure the spectrum of selectively reflected light over a wide wavelength and temperature range. Two types of apparatus were employed, (i) a Pye Unicam UV/Vis recording spectrometer, and (ii) a specially adapted microscope/hot stage system fitted with a spectrum analyzer. In the former case a modified Mettler FP82 hot stage was fitted into the sample chamber to allow the temperature of the liquid crystal to be varied between -60°C and 300°C at intervals of 0.1°C . In using the UV/Vis spectrophotometer, it was assumed that the selective reflection spectrum of the material was equivalent to the measured absorption spectrum. In the second system, an adapted Olympus BH2 Polarising Transmission/Reflection microscope was used in its reflection mode to illuminate the sample of chiral nematic material. The microscope modification, described in detail elsewhere,⁸ allowed light selectively reflected by the liquid crystal to be passed directly into a monochromator. This detector was linked to a BBC

microcomputer which allowed signal averaging and detailed spectral analysis to take place.

In both of these spectral analysis systems, the selective reflection spectra measured were broadened to some extent as a result of illumination and detection at non-normal incidence. However, for each of the systems described, it was possible to make a correction for the cone angle of light incident on the chiral nematic material to allow for the angular dependence of the selective reflection. This correction method has been described in detail elsewhere,⁸ and relies on the shift in wavelength, λ_o , to a lower value, λ_s , being related to the angles of the incident and reflected light (θ_i and θ_r) by the equation⁹

$$\lambda_s = \lambda_o \cos \frac{1}{2} \left[\sin^{-1} \left(\frac{\sin \theta_i}{\bar{n}} \right) + \sin^{-1} \left(\frac{\sin \theta_r}{\bar{n}} \right) \right]. \quad (3)$$

If it is assumed that, in the worst case, light is incident and detected from the extremes of the illuminating cone angle ($\sim 20^\circ$ and 14.5° , respectively, for the spectrophotometer and microscope optical systems), we obtain a correction factor which is dependent only on the average refractive index \bar{n} of the material. It should be noted that this correction factor is not exact as the above equation is valid only for small θ_i and θ_r . Nonetheless, it gives a useful correction to the measured spectra, decreasing the overall inaccuracy of wavelength measurements in the spectrophotometer and microscope systems to ± 4 nm and ± 3 nm, respectively.

3. THE INFLUENCE OF BIREFRINGENCE

3.1. Materials



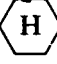
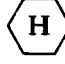
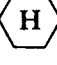
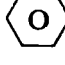
A series of liquid crystalline mixtures was made⁸ in which CB15, used as a twisting agent, was dissolved in several different nematic hosts. The chirality of the CB15 induced cholesteric phases in the mixtures and, at approximately 40% by weight of CB15, the selective reflection occurred in the visible region of the spectrum. The nematic hosts were chosen to produce chiral nematics exhibiting a wide range of birefringences. The compositions of the mixtures are given in Table I. The totally

TABLE I

The compositions of the chiral nematic materials and their racemic equivalents used in this study. BDH and Merck mixtures are marked (†) and (‡) respectively.

	Nematic Host % (by weight)	Nematic Host
CB15/CCH	62.3	ZLI1695‡
CB15R/CCH	62.5	ZLI1695‡
CB15/PCH	60.3	ZLI1132‡
CB15R/PCH	60.3	ZLI1132‡
CB15/E63	50.8	E63†
CB15R/E63	50.0	E63†

nematic equivalents of these cholesteric mixtures were also made using racemic CB15, denoted CB15R, in which the net chirality of the materials was zero. The compositions of these racemic mixtures are also given in Table I. All of the nematic hosts which were used are themselves mixtures and the nomenclature used in the table is that used by BDH⁷ and Merck.¹⁰ The materials were all obtained from BDH Ltd. and no attempt was made to purify them further. Differential scanning calorimetry on the base materials indicated their high degree of purity. One final mixture was made to extend the range of the birefringence of the cholesteric materials to very low values. The mixture was denoted 01/D3 and its composition together with the chemical structure of the constituent esters are given below. No racemic equivalent of the mixture 01/D3 was produced.

		01/D3
Osman (3/5)	C_3H_5  CO_2  C_5H_{11}	25%
Osman (5/5)	C_5H_{11}  CO_2  C_5H_{11}	25%
Demus	C_5H_{11}  CO_2  2Me*Bu	50%

3.2. Measurements of the Refractive Indices of the Cholesteric/Nematic Phases

The refractive indices of the liquid crystals were measured using an Abbé refractometer (Bellingham and Stanley Ltd., Tunbridge Wells, Kent, U.K.) in which alignment layers had been formed on the prisms of the apparatus to give the required orientation of the liquid crystal. The aligning agent used depended on the type of phase being studied; rubbed PVA gave uniform planar alignment for the cholesteric materials, while lecithin (BDH Egg Grade II) was used to align the nematic materials homeotropically. The temperature range of the refractive index measurements was from 14°C up to the Ch/N→I transition of each material. Temperature stability over this range was $\pm 0.5^\circ\text{C}$. The transition temperatures of the liquid crystals were determined optically using an Olympus BH2 polarizing microscope and Mettler FP82 hot stage, accurate to $\pm 0.1^\circ\text{C}$, and their values are given in Table II. The crystalline (or smectic) to cholesteric/nematic transition temperatures could not be measured for any of the materials containing CB15 or CB15R as these occurred below -60°C , which was the low temperature limit of the hot stage.

The temperature dependence of the refractive indices for each of the liquid crystalline materials studied is shown in Figure 1(a)–(d). All of the data were measured at 589.3 nm using a sodium lamp as the light source. In the figures, the measurements relating to the cholesteric phases and the equivalent nematic materials are presented together. The values of each of the refractive indices in the cholesteric phases, n_e and n_o , may be related to those measured in the refractometer, n_1 and n_2 , using the relationships¹¹ $n_{e,\text{Ch}} = n_1$ and $n_{o,\text{Ch}} = (2n_2^2 - n_1^2)^{1/2}$.

As may be seen from Figure 1(a)–(c), which refer to the materials CB15(R)/CCH, CB15(R)/PCH and CB15(R)/E63, respectively, these equations describe well

TABLE II

The transition temperatures of the mixtures CB15(R)/CCH, CB15(R)/PCH, CB15(R)/E63 and 01/D3. The refractive indices, n_o and n_e , birefringence and average refractive index measured at 20°C are also shown.

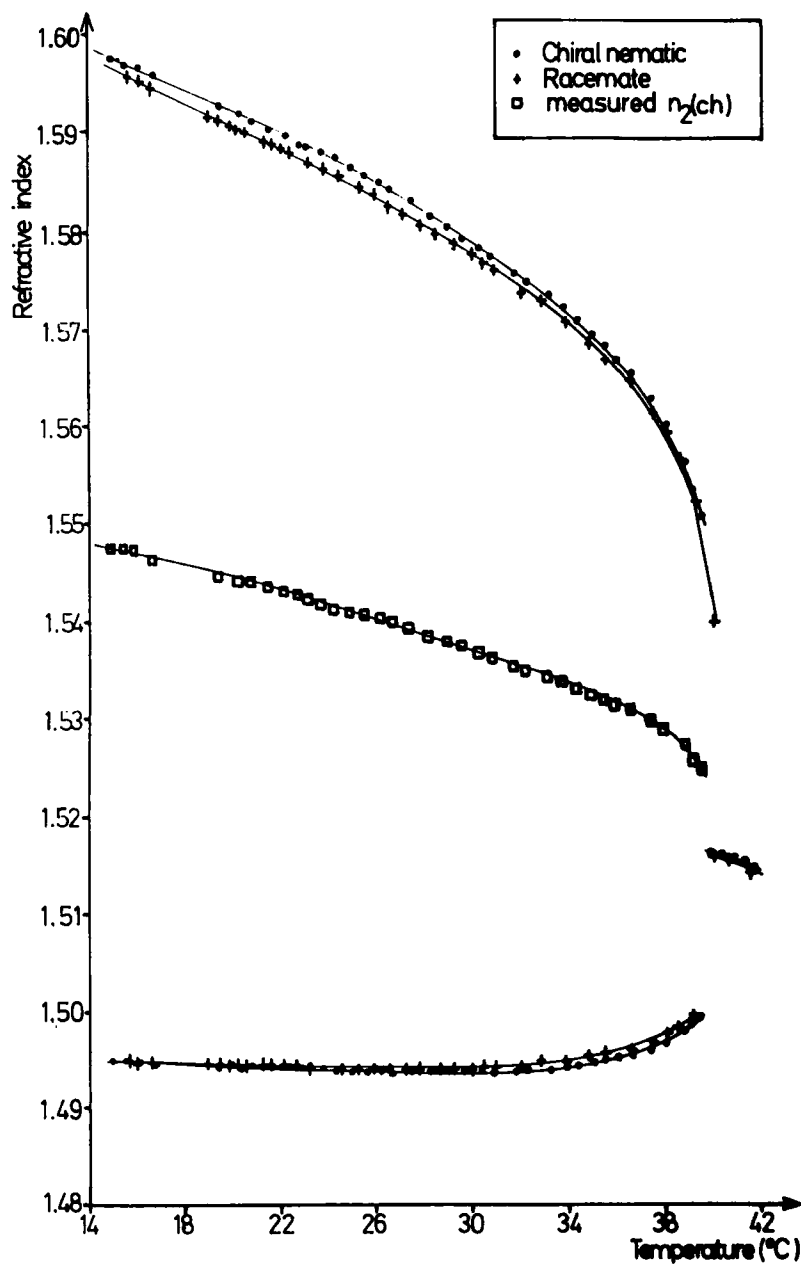
	K/S→Ch/N (°C)	Ch/N→I (°C)	n_o	n_e	\bar{n}	Δn
CB15/CCH	< -60°C	41.7	1.496	1.591	1.544	0.095
CB15R/CCH	< -60°C	41.2	1.495	1.592	1.544	0.097
CB15/PCH	< -60°C	38.1	1.517	1.647	1.582	0.130
CB15R/PCH	< -60°C	39.2	1.515	1.653	1.584	0.138
CB15/E63	< -60°C	37.7	1.541	1.697	1.619	0.156
CB15R/E63	< -60°C	36.3	1.541	1.695	1.618	0.154
01/D3	9.1(S _B)	27.1	1.473	1.513	1.493	0.040

the refractive indices in the cholesteric phase. The small differences (<0.1%) which are observed between the refractive indices of the cholesteric phase and their racemates at equivalent temperatures may be attributed to two effects. The first is due to the small differences in composition between the materials (as given in Table I), and the second is due to the slight difference in transition temperatures (see Table II) always observed between a cholesteric material and its racemate.¹² The values determined for CB15/PCH and CB15R/PCH which have exactly the same composition can be seen to agree extremely well [Figure 1(b)] if the small temperature shift is taken into account. The mean refractive index \bar{n} and the birefringence Δn for each of the chiral nematic materials are shown as a function of temperature in Figure 2(a) and (b), respectively. It can be seen that the mixtures studied cover a range of \bar{n} from 1.49 to 1.62 and Δn from 0.04 to 0.16. The transition temperatures, together with the refractive indices of each of the materials at 20°C are given in Table II for comparison.

The spectrum of the selectively reflected light was determined⁸ for each of the chiral nematic materials from 14.0°C up to the chiral nematic (or nematic) to isotropic phase transition at temperature intervals of 1.0°C. For each of the spectra recorded, the values of λ_p and $\Delta\lambda$ were measured, Figure 3(a) and (b), respectively, and $\lambda_p/\Delta\lambda$ calculated, Figure 4(a)–(d). These data are presented and discussed in the following section where a direct comparison of the values of $\lambda_p/\Delta\lambda$ and $\bar{n}/\Delta n$ is made.

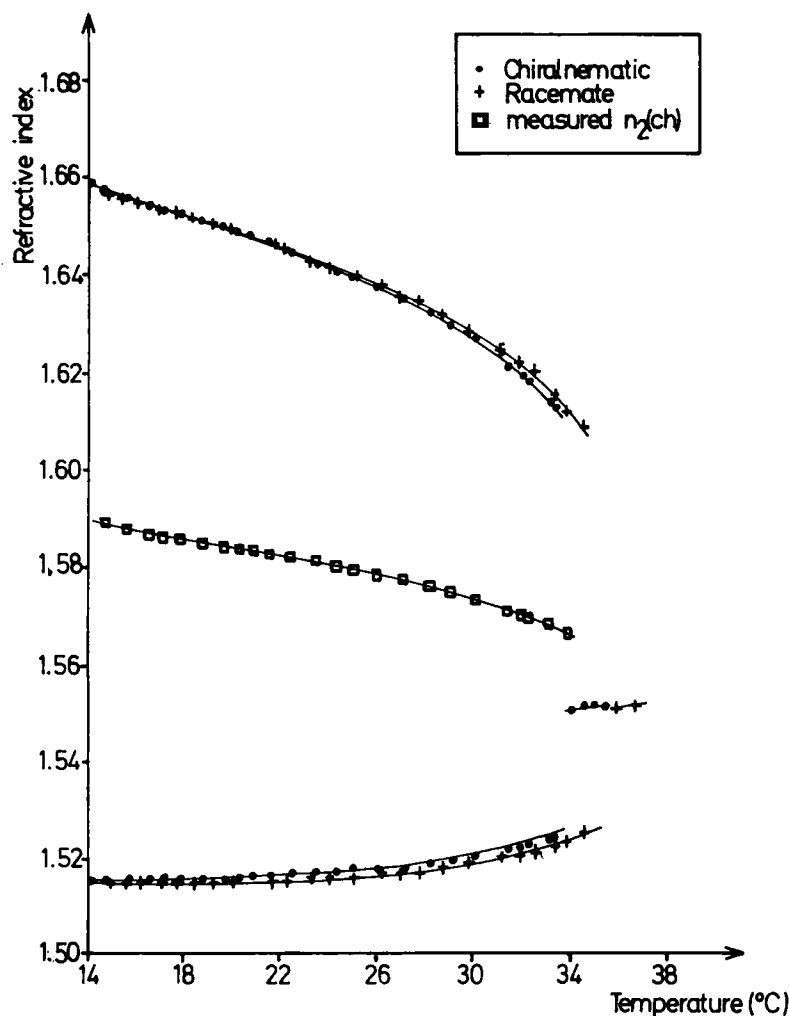
3.3. Results and Discussion—Birefringence

The refractive index and birefringence data, Figure 2(a) and (b) show clearly the wide range of \bar{n} and Δn available with the mixtures studied. Although in this study we are primarily interested in the validity of the de Vries equations, through the behavior of $\bar{n}/\Delta n$ and $\lambda_p/\Delta\lambda$, it is important to note that both \bar{n} and Δn are temperature-dependent, albeit only weakly so, in the case of \bar{n} . Our original⁸ selective reflection data on these wide refractive index and birefringence range mixtures has



(a)

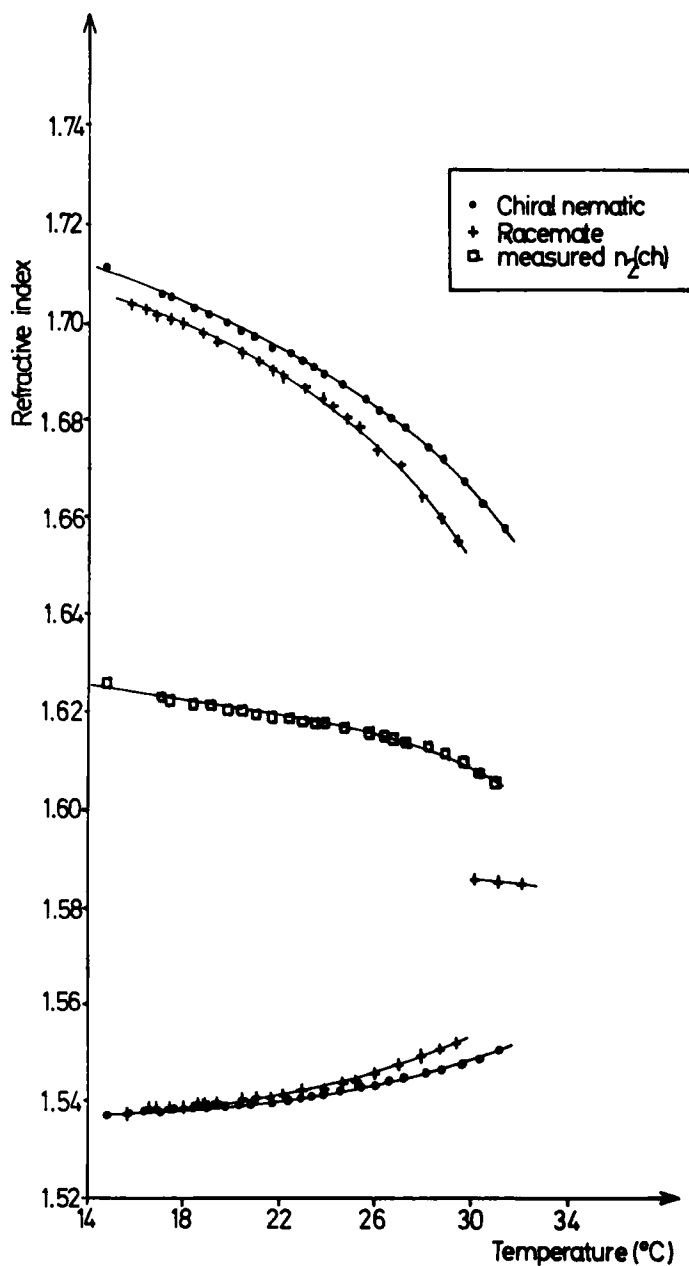
FIGURE 1 The refractive indices of the chiral nematic mixtures (a) CB15/CCH, (b) CP15/PCH, (c) CB15/E63 and their racemates, and (d) 01/D3 as a function of temperature. In the case of the chiral nematics, the measured parameter n_2 is also shown.



(b)

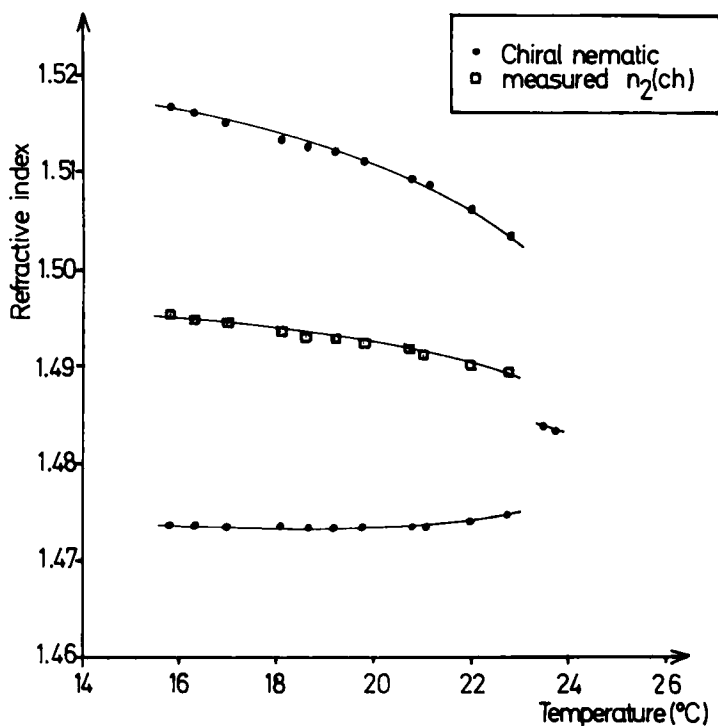
FIGURE 1 (continued)

been confirmed⁴ in a parallel study using CB15 as a twisting agent in related CCH and PCH mixtures. As noted in Reference 4 the highly dipolar mixtures based on CB15 show an unusual linear increase in λ_p with increasing temperature, whereas the ester mixture 01/D3, without the strong cyano dipole, shows a more normal decrease in λ_p with increasing temperature as the transition to the isotropic phase is approached, Figure 3(a). The reflection spectrum peak width $\Delta\lambda$ is also temperature dependent, Figure 3(b), although the data for the CB15 based mixtures considered here are grouped around a higher mean $\Delta\lambda$ (~ 40 nm) than the ester mixtures (~ 10 nm).



(c)

FIGURE 1 (continued)



(d)

FIGURE 1 (continued)

From the above data it is clear that λ_p , $\Delta\lambda$, \bar{n} and Δn are all dependent to a greater or lesser extent on temperature and mixture composition. It is worth noting that for the materials doped with CB15, since the temperature dependence of both λ_p and \bar{n} is essentially linear in the temperature range examined, it is, in principle, possible to consider the interdependence of $\Delta\lambda$ and Δn directly. However, this is not always the case, and in general, in order to examine the behavior of the de Vries equations further, we must examine the behavior of both $\lambda_p/\Delta\lambda$ and $\bar{n}/\Delta n$ separately. The independently measured parameters $\lambda_p/\Delta\lambda$ and $\bar{n}/\Delta n$ are shown over a wide temperature range for each of the liquid crystal mixtures in Figure 4(a)–(d) which refer to CB15/CCH, CB15/PCH, CB15/E63 and 01/D3, respectively. It can be seen from Figure 4 that, although for each material the form of the curves describing $\lambda_p/\Delta\lambda$ and $\bar{n}/\Delta n$ is the same, the graphs do not exactly coincide. Furthermore, the difference between the values of $\lambda_p/\Delta\lambda$ and $\bar{n}/\Delta n$ becomes larger as the birefringence of the material becomes smaller (values agree to within 5% for $\Delta n > 0.1$, but only to within 25% for $\Delta n \sim 0.05$). It is interesting to consider the possible origins of the differences.

The small differences observed between $\lambda_p/\Delta\lambda$ and $\bar{n}/\Delta n$ might be attributable to several different factors. First, the maximum uncertainty in the measurement of wavelength (± 3 nm) which occurs using the apparatus described can introduce

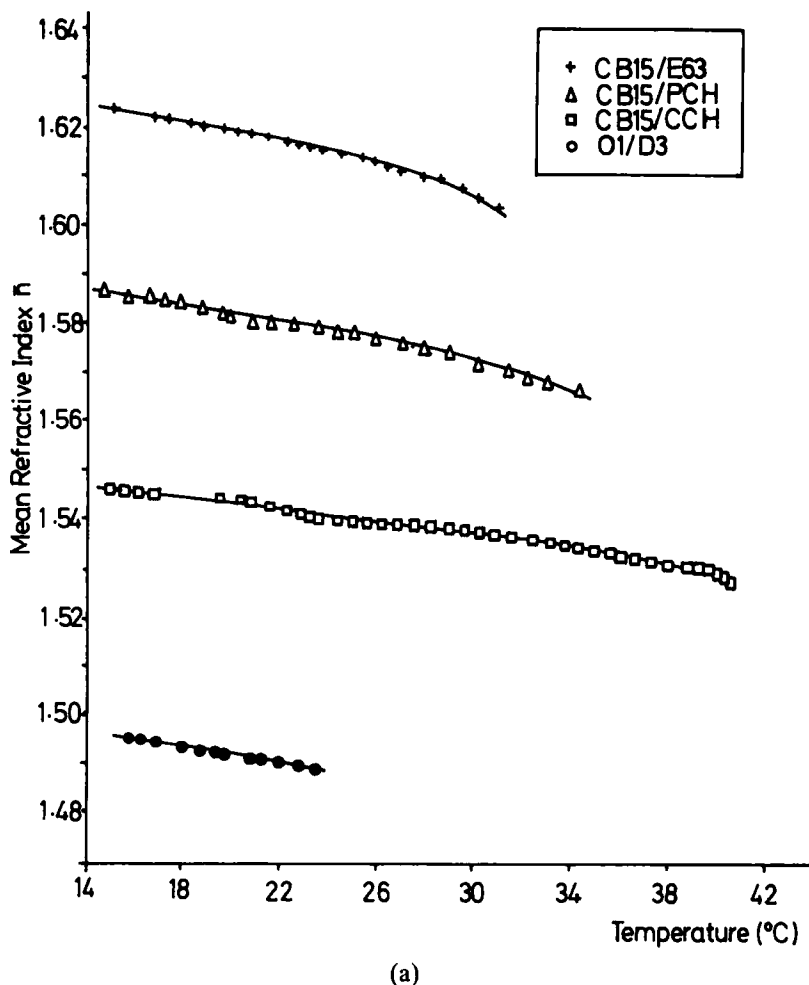
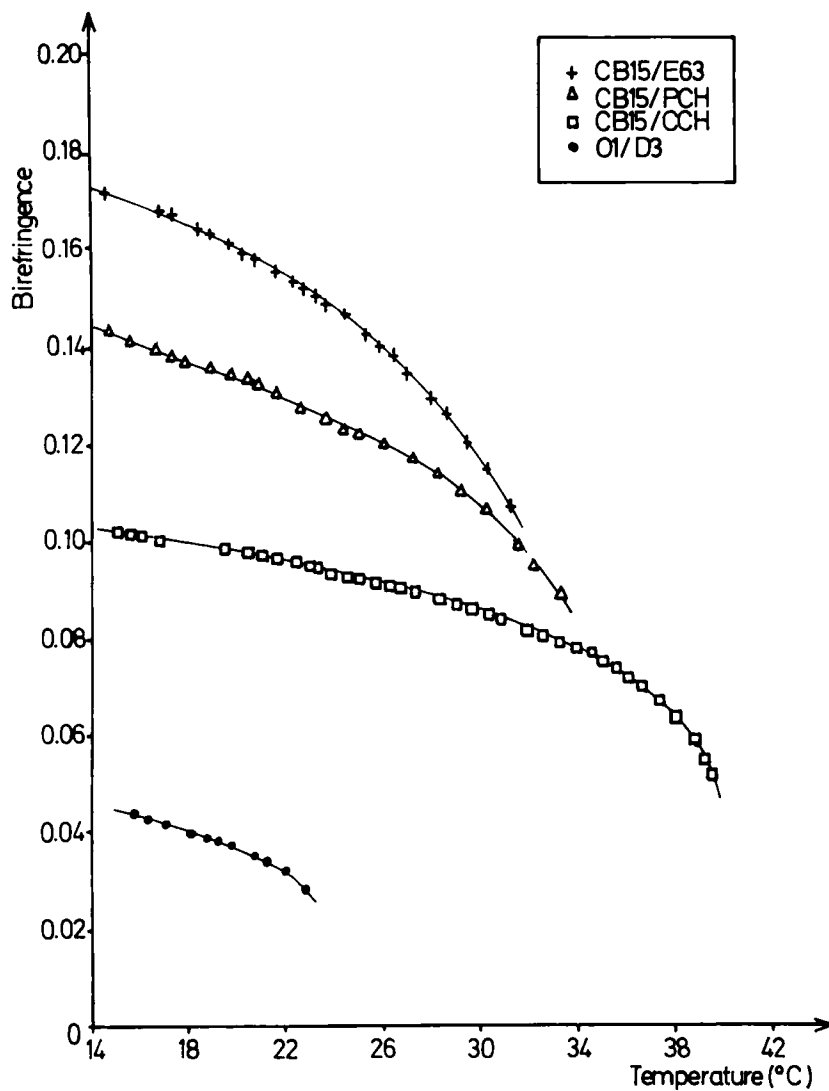


FIGURE 2 The temperature variation of (a) the mean refractive index, and (b) the birefringence of the chiral nematic mixtures CB15/CCH, CB15/PCH, CB15/E63 and 01/D3 as measured using an Abbé refractometer.

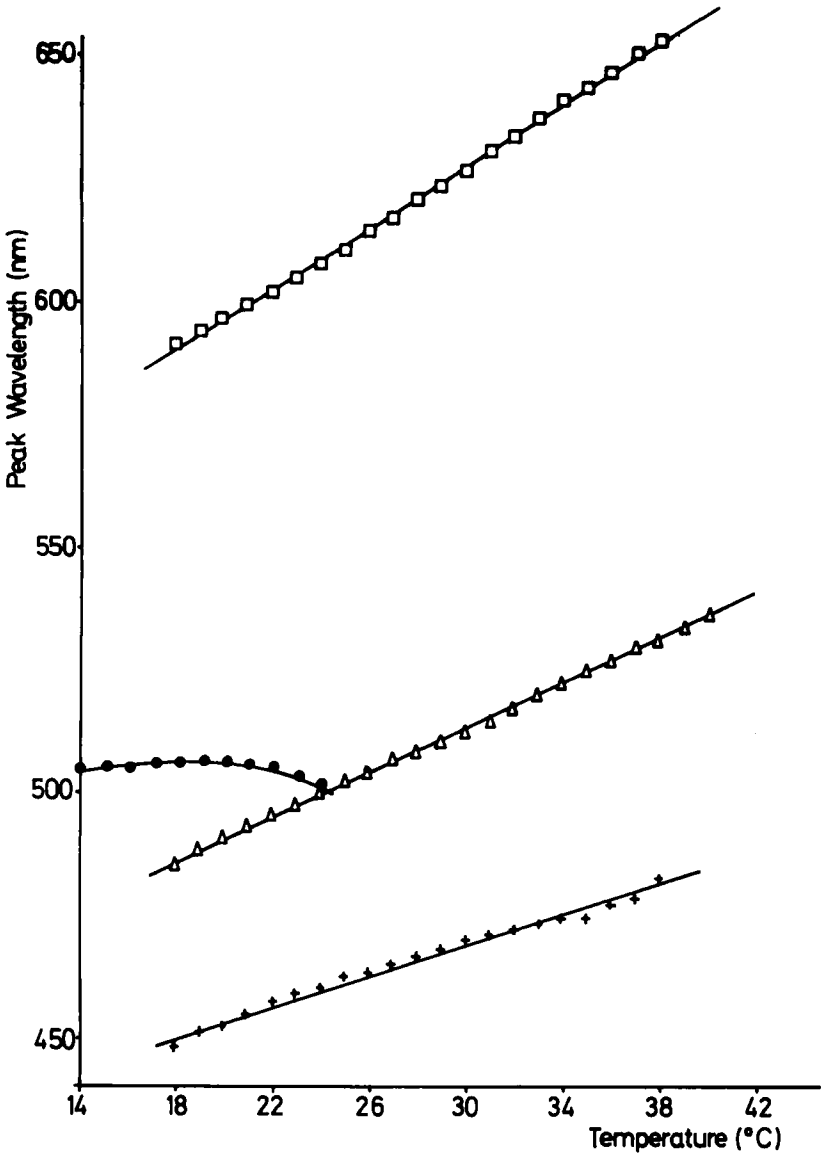
errors in $\lambda_p/\Delta\lambda$ which appear relatively large for the low birefringence materials. In fact, at 20°C the upper and lower limits of $\lambda_p/\Delta\lambda$, calculated from the experimentally determined data, bracket the average value by 2.5, 2.6, 3.1 and 60 units for CB15/E63 ($\Delta n = 0.156$), CB15/PCH ($\Delta n = 0.13$), CB15/CCH ($\Delta n = 0.09$) and 01/D3 ($\Delta n = 0.04$), respectively. The large uncertainty in $\lambda_p/\Delta\lambda$ for 01/D3 occurs because the denominator, $\Delta\lambda$, is small (~ 10 nm) and comparable to the measurement uncertainty for this material. It is important to note, however, that such a source of measurement error would be random in nature and the data should therefore be scattered randomly around an average value. There is no evidence of this in our results (Figure 4). Second, in calculating the cone angle correction used in wavelength measurements for each material, the value of the average refractive



(b)

FIGURE 2 (continued)

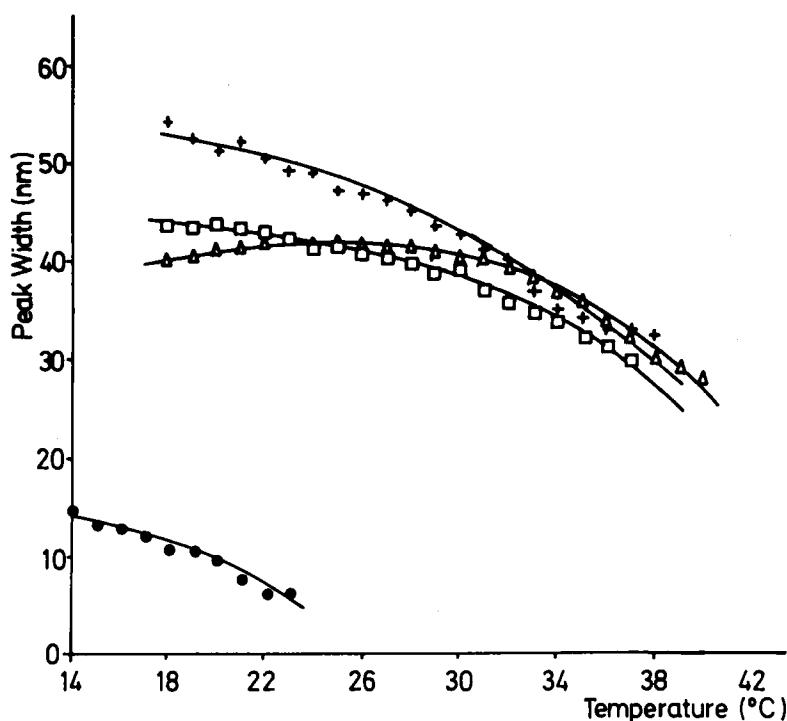
index \bar{n} at 20°C was used over the whole chiral nematic range. However, it can be seen from Figure 2(b) that \bar{n} is not a constant, and variation of \bar{n} with temperature might possibly account for the crossovers of the graphs of $\lambda_p/\Delta\lambda$ and $\bar{n}/\Delta n$ seen in Figure 4(a) to (d) (CB15/CCH, CB15/PCH and CB15/E63). Third, it is possible that there is a systematic error in the values of the cone angles used in the correction factor. Again, the effect of this would dominate in the low birefringence materials where the percentage difference due to a small error such as this becomes larger.



(a)

FIGURE 3 The temperature variation of (a) the peak selectively reflected wavelength λ_p , and (b) the peak width $\Delta\lambda$ of the mixtures CB15/CCH, CB15/PCH, CB15/E63 and 01/D3. Symbols key as for Figure 2.

The influence of these last two possible sources of experimental error (i.e., variation of \bar{n} and a different cone angle) can be seen in Figure 4(a), marked by the triangle and square, respectively. The effects on the calculated values of $\lambda_p/\Delta\lambda$ made by including the maximum extra small corrections in the values of \bar{n} and the cone angle of the incident light are clearly very small, changing $\lambda_p/\Delta\lambda$ by $\sim \pm 0.2\%$,



(b)

FIGURE 3 (continued)

and so cannot satisfactorily account for the differences seen in the graphs of $\lambda_p/\Delta\lambda$ and $\bar{n}/\Delta n$.

Having considered both the origins and the influence of all the experimental errors in our measurements, we conclude that the differences observed in $\lambda_p/\Delta\lambda$ and $\bar{n}/\Delta n$ for low birefringence materials and the crossover are real. Nevertheless, these differences are small, and we may further and more importantly conclude that Equation (2) holds well for the large birefringence, new chiral nematic mixtures discussed. Although the form of the graphs of $\lambda_p/\Delta\lambda$ and $\bar{n}/\Delta n$ are the same for all the mixtures, the equivalence is not proven for low birefringence ($\Delta n = 0.04$) materials. In the only other parallel study⁴ on similar mixtures with low Δn materials, the dependencies of \bar{n} and Δn on temperature were not considered and so no further comparison to the present work is possible. However it is worth remarking that the expression $\Delta\lambda = \Delta n \lambda$ given in Reference 4 is incorrect and should contain the term in \bar{n} given in Equation (2). This is important since, as shown in Figure 2(b), \bar{n} , which is weakly temperature dependent, may be varied by changes in mixture composition. Thus both Δn and \bar{n} , as well as λ_p , influence the final value of $\Delta\lambda$ at a given temperature.

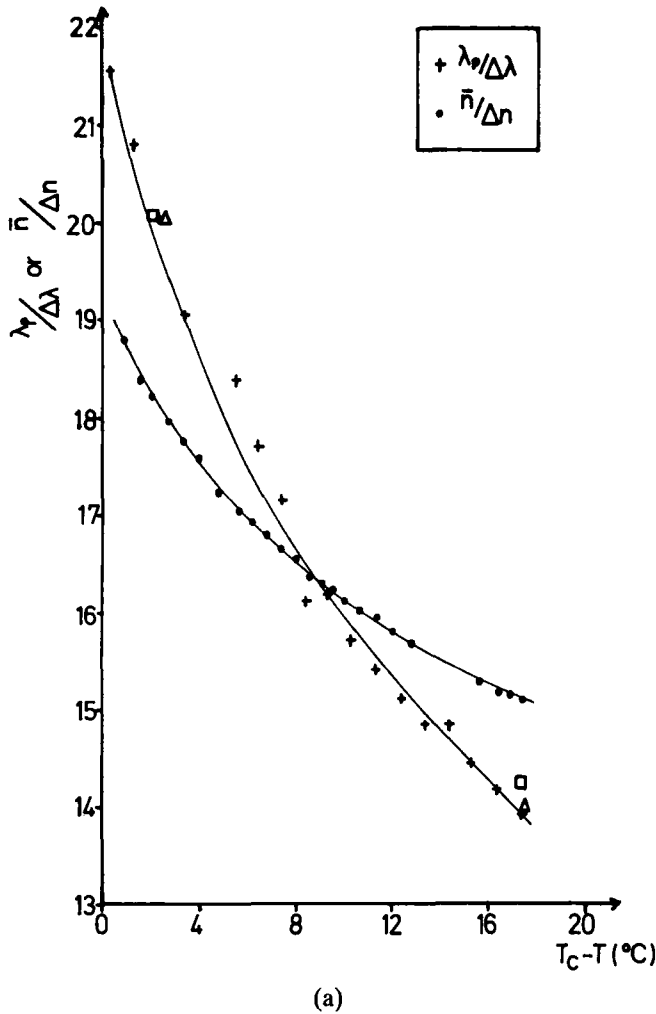


FIGURE 4 A comparison of the independently measured ratios, $\lambda_p/\Delta\lambda$ and $\bar{n}/\Delta n$, for the mixtures (a) CB15/CCH, (b) CB15/PCH, (c) CB15/E63 and (d) 01/D3 with respect to the temperature difference from the clearing point. In Figure 4(a) the triangles (Δ) refer to the points for which the average refractive index \bar{n} has been corrected, while the squares (\square) refer to points where the cone angle has been changed from 14.5° to 16° (see text).

4. THE INFLUENCE OF THE TWISTING POWER

4.1. Materials

In order to investigate the influence that variation in twisting power of a chiral nematic material has on properties of the mesophase, it was important to study a series of materials in which the only adjustable parameter was the chirality. This was done by preparing a series of mixtures which consisted of a chiral base to which increasing amounts of racemic material were added, thereby progressively increas-

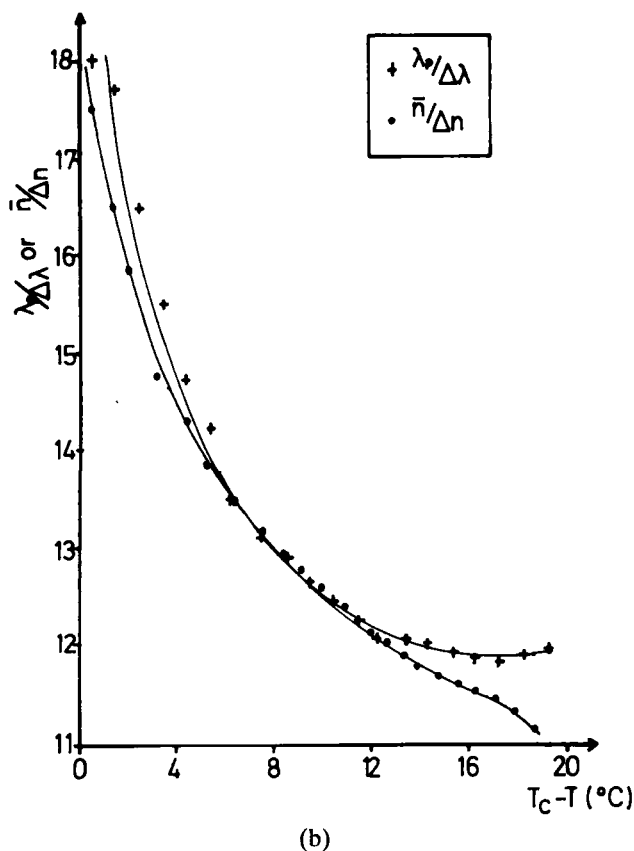
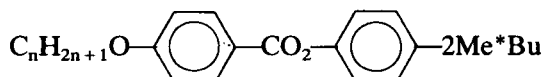


FIGURE 4 (continued)

ing the pitch of the mesophase at constant temperature without changing Δn or \bar{n} , in contrast to Section 3.2. In these mixtures the chiral base, denoted HG1 was composed of CE4, CE5 and CE6 in the proportions 40.0%, 30.0% and 30.0% by weight, respectively. The nomenclature is that used by BDH Ltd.,⁷ and the structures of the materials are shown below where $n = 6, 8$, and 10 correspond to CE4, 5 and 6, respectively.

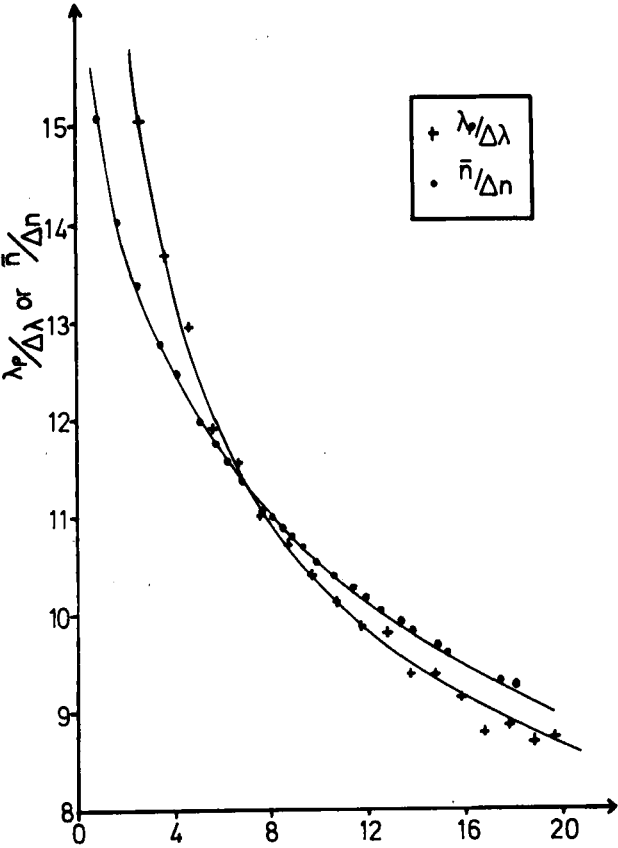


The composition of the mixtures which contained increasing proportions in the racemate of the chiral base are shown in Table III. This table also includes the transition temperatures of the mixtures determined by optical microscopy with an accuracy of $\pm 0.1^\circ\text{C}$. It can be seen from the table that the transition temperatures of the materials increase slightly as the proportion of racemic material in the mixture increases, as expected.¹²

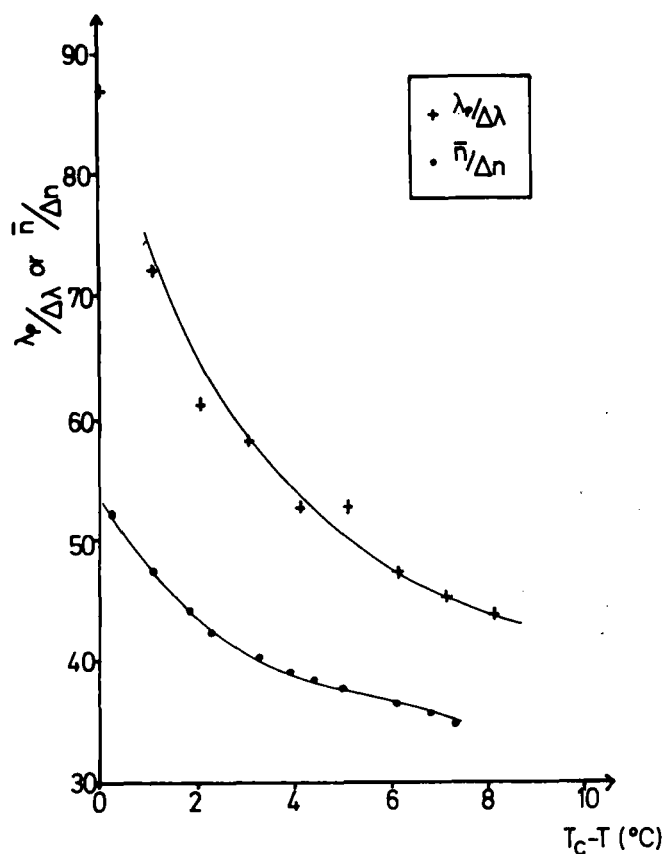
TABLE III

The proportion of racemic material induced in the chiral nematic mixtures of this study and their transition temperatures.

	HG1R % (w/w)	S _A →Ch (°C)	Ch→I (°C)
HG1	0	27.4	40.4
HG1R10	11.3	27.8	40.5
HG1R20	22.1	28.0	40.7
HG1R30	29.5	28.1	40.8
HG1R40	40.2	28.2	40.9
HG1R	100	28.4	40.9



(c)
FIGURE 4 (continued)



(d)

FIGURE 4 (continued)

It should be noted that the small change in transition temperature from mixture to mixture could be expected to influence a direct comparison of the selective reflection spectra of the different materials. This is especially true close to the cholesteric to smectic transition where the pitch of the cholesteric mesophase diverges rapidly. In this temperature region, even a small difference in transition temperature would result in a dissimilarity in the properties of each mixture at a specific temperature, since the asymptote of the divergence has effectively been moved. This feature of the mixtures will be discussed more fully when the pitches of each of the materials are compared below through the measurement of λ_p .

4.2. Results and Discussion

The experimentally determined color-play of each of the mixtures over the range of the chiral nematic phase is shown in Figure 5. As the proportion of racemate in the ester mixture was increased, the twisting power of the material became smaller, and for a given temperature the selective reflection peak moved toward

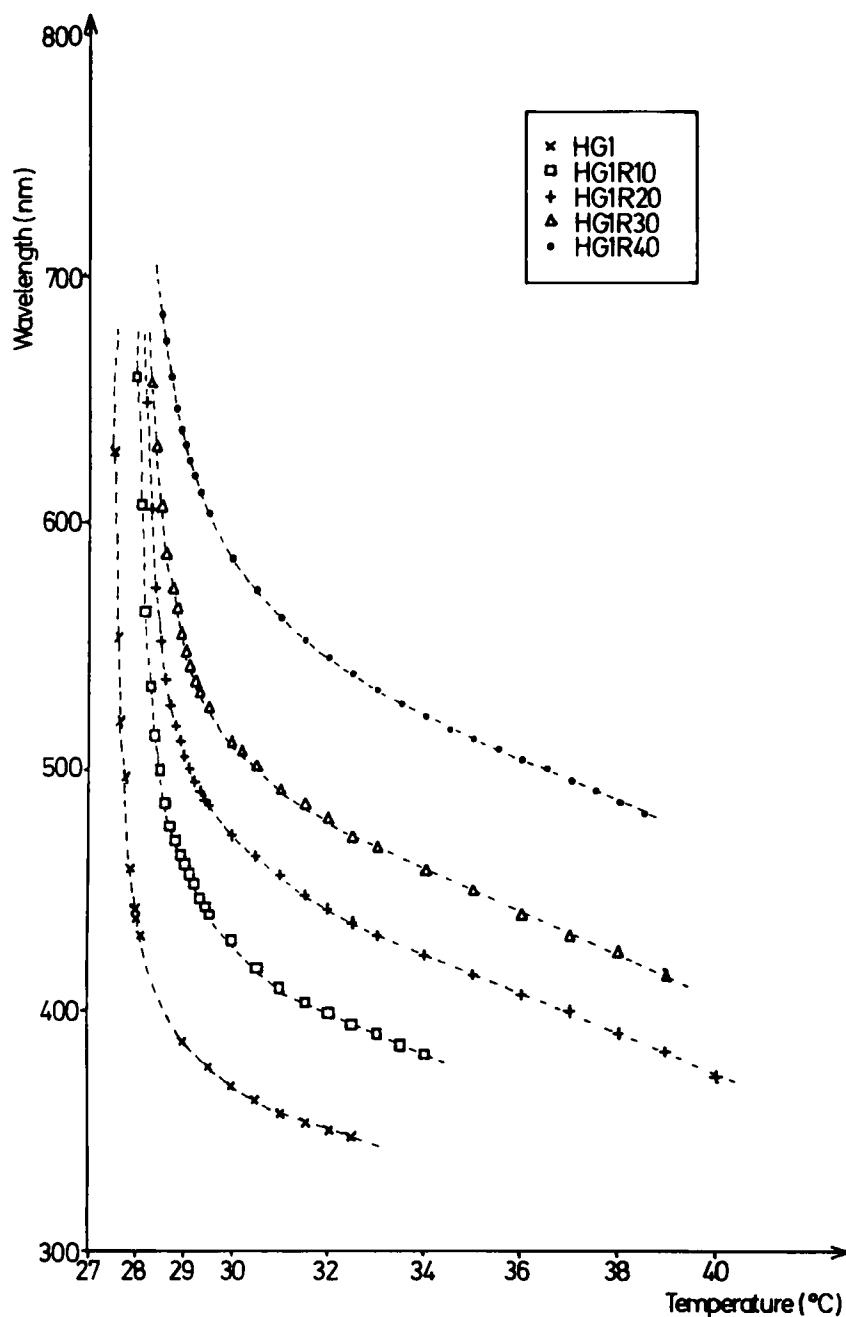


FIGURE 5 The experimentally determined temperature variation of λ_p in the series of materials HG1, HG1R10, HG1R20, HG1R30 and HG1R40.

the red end of the spectrum. The diagram also illustrates the divergence of the pitch in the cholesteric mesophase as the smectic transition is approached. It can be seen that the asymptote of this divergence occurs close to the Ch→S transition temperature, which increases with increasing proportion of racemate and shows clearly the effect of the decrease in the twisting power.

It can also be seen from Figure 5 that the shape of the peak wavelength versus temperature curve changes, particularly close to the $S_A \rightarrow Ch$ phase transition, as the twisting power of the material is varied, in common with the color play curves of the BDH mixtures TM74A + B and TM75A + B¹³ which also have the chiral esters CE4, -5 and -6 among their components. Although such behavior is well known, the effect (if any) that this decrease in twisting power has on the form of the critical divergence of pitch with temperature has not previously been quantified. In these materials, the functional dependence of the wavelength on temperature appears to become less divergent in the visible spectral range as an increasing amount of racemic material is added to the mixtures, Figure 5. However, it can be shown that this is simply due to a shift of the color play curve to longer wavelengths and that the functional dependence of peak wavelength on temperature is equivalent for each of the mixtures.

The pitch of a mixed system of liquid crystals is given by,¹⁴

$$\frac{1}{p_t} = \sum_i \frac{c_i}{p_i},$$

where p_t is the pitch of the final mixture, and c_i and p_i the weight percentage and pitch at a given temperature for the individual components, respectively. For this series of ester mixtures, the pitch of the racemates may be assumed to be infinite. The above equation holds unless the constituent molecules in the mixture are dissimilar, when mutual molecular interactions may cause anomalous behavior, as in the case where injected smectic phases occur in binary mixtures.^{15,16} Using the above equation, together with Equation (1), i.e., $\lambda_p = \bar{n}p$, the color play of each of the ester materials may be predicted from the data of any one of the other mixtures. It should be noted that for this series of materials \bar{n} is constant between the mixtures at each specific temperature.

A comparison between the actual and predicted data is shown in Figure 6(a) and (b). Using $1/p_t = \sum_i c_i/p_i$, [Equation (1)], and the data of Table III, it can be easily shown that at each temperature,

$$\lambda_o = \frac{\lambda_{10}}{1.13} = \frac{\lambda_{20}}{1.28} = \frac{\lambda_{30}}{1.42} = \frac{\lambda_{40}}{1.67}$$

where the subscript denotes the mixture being considered (i.e., λ_{10} refers to HG1R10, etc.). It can be seen that the form of the curves exhibited by the actual data [Figure 6(a)] are qualitatively reproduced in Figure 6(b) where each of the data points on the curves has been calculated using the above relationship from the data for HG1.

A more complete comparison between the measured and predicted data was also made for each of the mixtures. The result for HG1R10 is shown in Figure 7, and

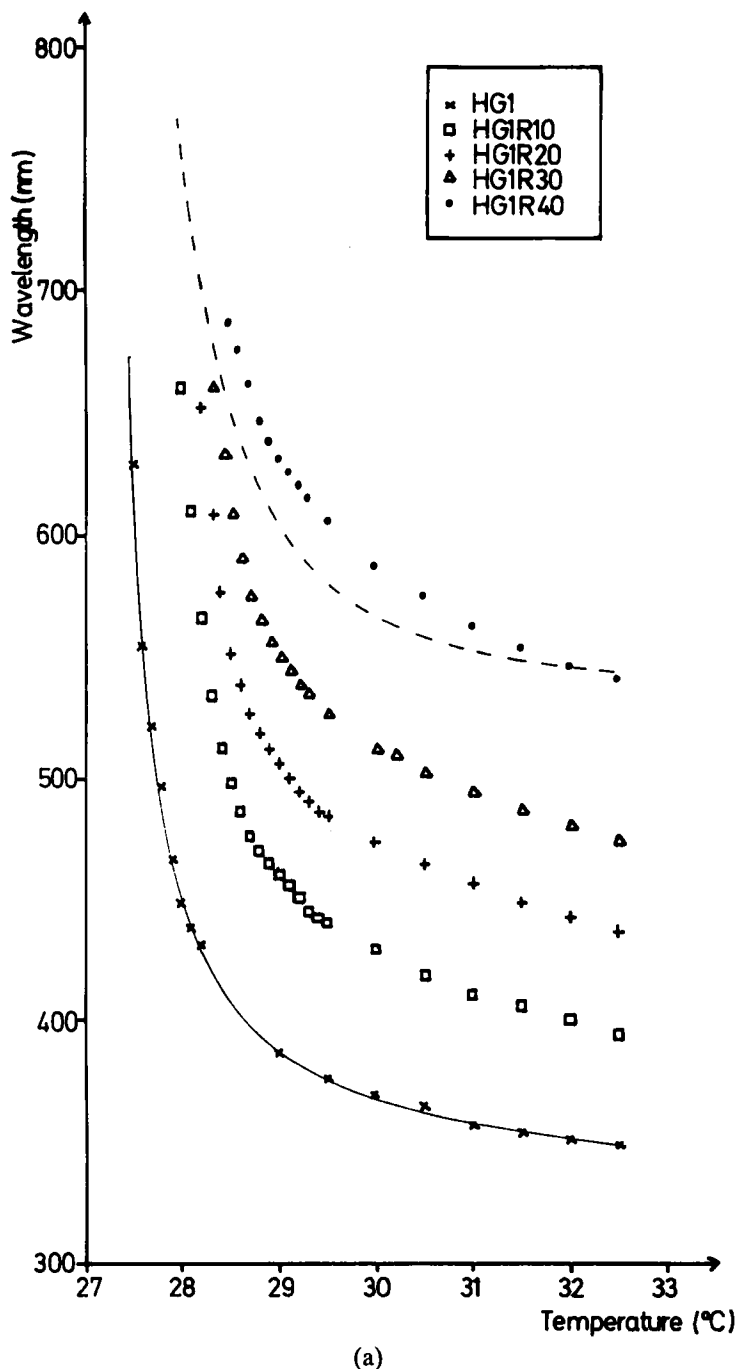
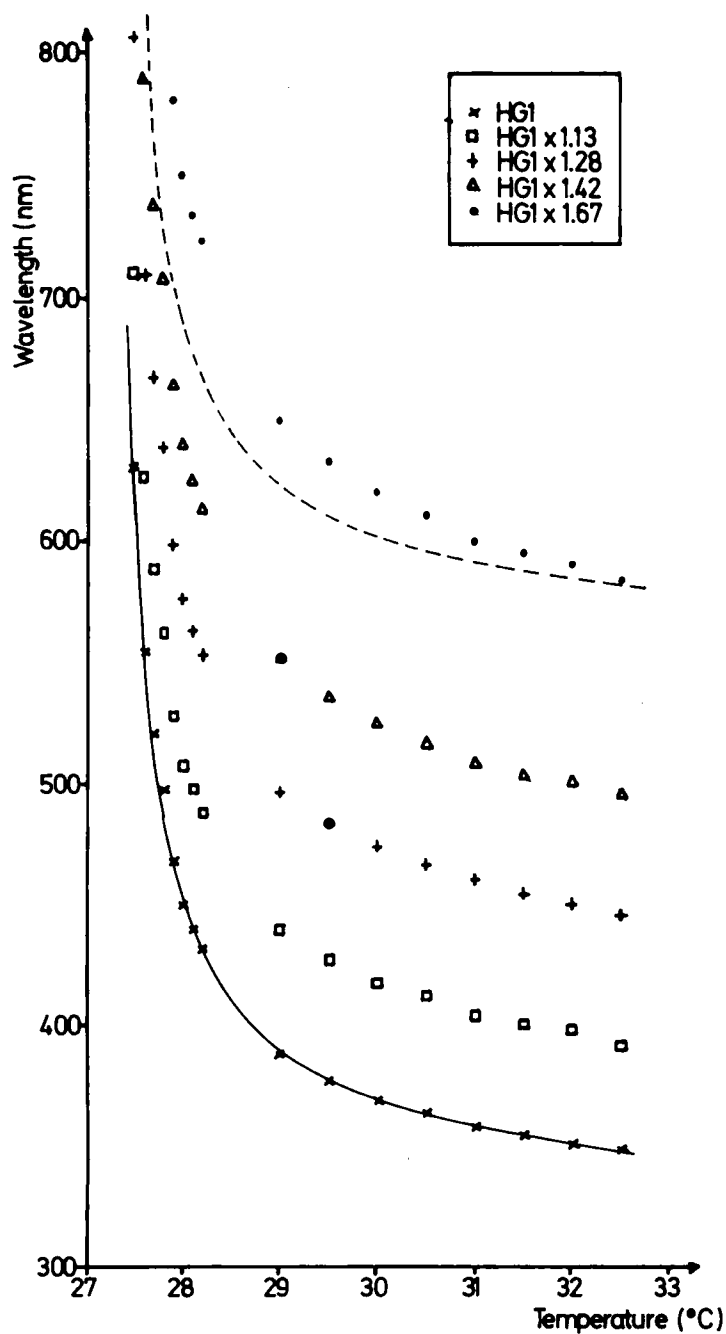


FIGURE 6 (a) The *experimentally* determined temperature dependence of λ_p for the HG1 series of mixtures over the range 27.0°C to 33.0°C, and (b) the variation *predicted* using the equation $1/p_i = \sum c_i/p_i$ and the data of HG1. The dashed lines in the figures represent the data of HG1 shifted in both wavelength and temperature to give the best possible fit to the actual and calculated data for HG1R40. In each case it can be seen that an increase in the pitch appears to make λ_p versus temperature less divergent at the $S_A \rightarrow Ch$ phase transition.



(b)

FIGURE 6 (continued)

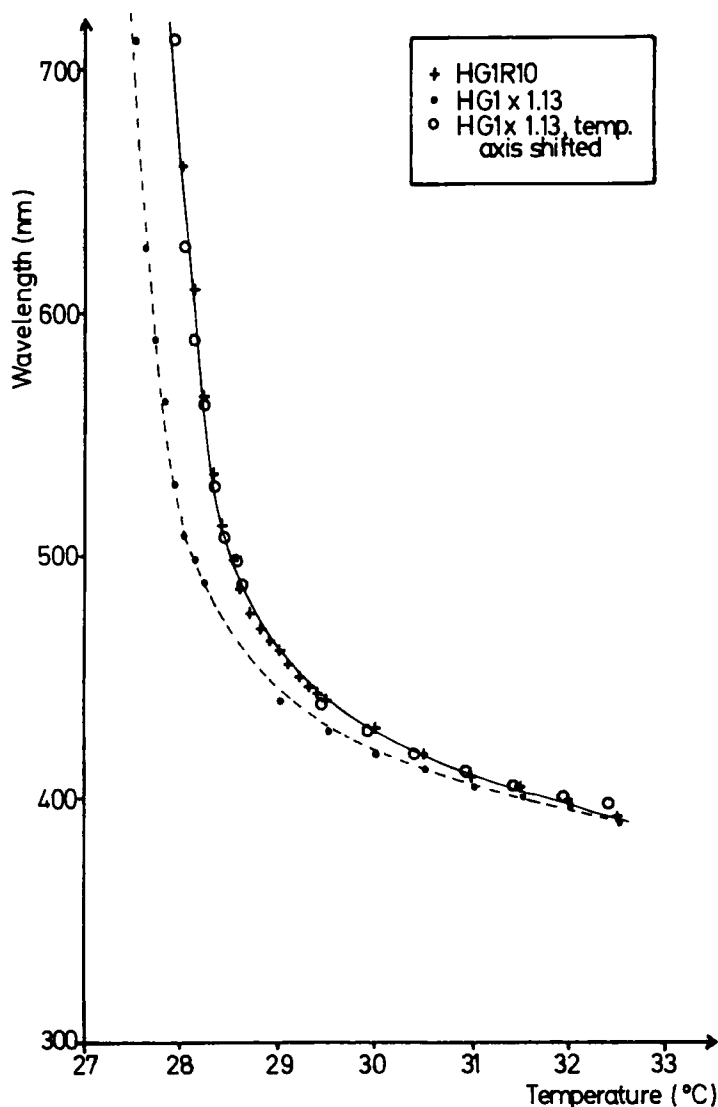


FIGURE 7 A comparison between the measured and predicted temperature dependence for HG1R10. The broken line corresponds to data predicted by calculation from HG1, but in which the transition temperature has *not* been shifted. Note the excellent agreement between the measured and calculated data where the increase in transition temperature has been taken into account.

the behavior seen is typical of all of the materials. The predicted data do not fit the measured wavelengths until the temperature axis is shifted to compensate for the increased transition temperature of HG1R10 above that of HG1 (i.e., by 0.4°C). Then the predicted data agree extremely well with those measured. It is not surprising that such a temperature shift is necessary before the model fits the experimentally observed data since the simple calculation described above cannot take into account the increased transition temperatures observed in the less twisted

mixtures. However, the fact that the temperature-shifted data agree so well with those predicted indicates that the change in initial pitch is not altering the functional dependence of the critical divergence of the peak wavelength with temperature. It can be shown, as follows, that the functional dependence of λ_p on temperature is indeed identical for each of the mixtures, confirming this postulation. In Figure 8 a series of curves is shown which have been calculated using the equation for the pitch proposed by Keating.¹⁷ It is noted that other dependencies of λ_p on temperature, such as that suggested by Alben¹⁸ might have been used instead of Keating's description. Elser and Ennulat¹⁹ have shown that both describe the variation of λ_p on temperature at the Ch-S_A transition equally well. The curves in Figure 8 are related to the actual experimental data in that the curve of largest twisting power, A, is that obtained when the wavelength/temperature data for HG1 were fitted to Keating's equation by computer over a temperature range of 2.3°C above the Ch→S phase transition. The equation which best fits the experimentally determined data is:

$$\lambda_{OF} = \frac{8852}{T} \left(1 + \frac{0.168}{T-27.4} \right)^2 \text{ (nm)}. \quad (4)$$

The subscript, OF, denotes the computer fitted dependence of λ_o on temperature. The curves B, C, D and E in Figure 8 (equivalent to HG1R10, HG1R20, HG1R30 and HG1R40, respectively) were calculated from the values of wavelength given by the above equation, using

$$\lambda_{OF} = \frac{\lambda_{10}}{1.13} = \frac{\lambda_{20}}{1.28} = \frac{\lambda_{30}}{1.42} = \frac{\lambda_{40}}{1.67}.$$

It can be seen that the fundamental dependence of wavelength on temperature remains the same for each of the curves in Figure 8. The curves in this figure again mimic the behavior of those shown in Figure 6(a) and 6(b) in that the materials with smallest twisting power appear to exhibit a less divergent color play. It is clear that a decrease in the twisting power of a material does not change any of the constants of Equation (4), but increases the selectively reflected wavelength at each temperature by a specific amount related directly to the increase in the helical pitch of the system. Thus, while a decrease in the twisting power of a material seems to linearize the temperature dependence of the selectively reflected wavelength peak, in fact the functional dependence is not changed. Furthermore, the shape of the curves may be predicted using a simple pitch calculation, remembering that the transition temperature of a mixture is likely to shift as increasing amounts of racemic material are added to it.

5. CONCLUSIONS

We have described materials and measurements which have allowed us to assess independently the influence of the birefringence and twisting power on the spectral characteristics of chiral nematic materials in accordance with de Vries's equations.

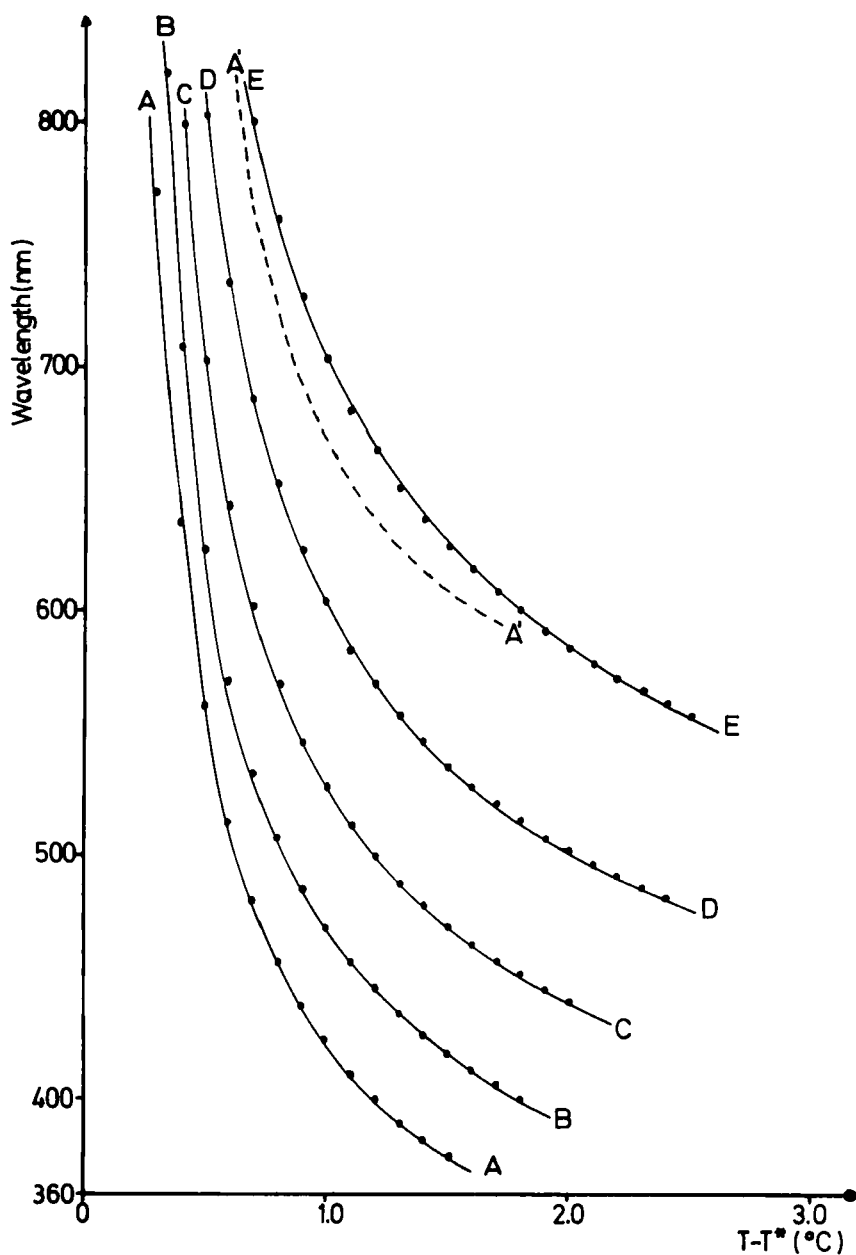


FIGURE 8 The *completely* theoretically determined wavelength, λ_{OF} , versus temperature dependence calculated from the Keating equation and derived initially from values of HG1. The letters A-E relate to the color plays predicted to be analogous to HG1, HG1R10, HG1R20, HG1R30 and HG1R40, respectively. The broken lines—A—shows the best fit of curve A to E. The form of these graphs can be seen to be equivalent to those of Figure 6(a), which is purely experimentally-determined data.

We conclude that (i) mixtures may be formulated with birefringences in the range $0.04 \leq \Delta n \leq 0.16$, (ii) \bar{n} and Δn may be measured independently of λ_p and $\Delta\lambda$, (iii) de Vries's Equation (2) holds well for large values of Δn but there are deviations for low Δn , (iv) the influence of variation in twisting power may be taken into account using a simple equation, and (v) neither the birefringence nor twisting power affect the temperature dependence of λ_p . It is clearly possible to modify the spectral characteristics and therefore the color purity, temperature resolution and brightness of thermochromic liquid crystals in a well controlled way. Manipulation of the birefringence alone may be achieved by dissolving the same chiral host in numerous nematic solvents. Addition of purely racemic material allows an independent variation of the pitch, and therefore λ_p . A combination of these two results thus allows the optical properties of a thermochromic material to be "tuned" to give the required λ_p , \bar{n} , Δn and therefore $\lambda_p/\Delta\lambda$ for a specific application. For example, where a bright device is required, the birefringence should be kept large, and the value of λ_p may be varied by adding racemic material. Alternatively, high accuracy thermometry or narrow band optical filters will depend upon low birefringence materials. Such thermometry devices will be necessarily less bright. It is important to note that the actual selection of mixtures for particular applications is somewhat more complicated as almost all devices include microencapsulated or polymer-dispersed liquid crystals, where the ability to vary \bar{n} over a wide range allows refractive index mismatching, and therefore light scattering, to be reduced at the liquid crystal/polymer interface. This improves further the perceived brightness of the specularly reflected light from the device. Also, in practical devices the randomly-oriented thermochromic droplets distort the selective reflection spectra further from the case described for a planar sample at normal incidence in Equations (1) and (2). Nevertheless, the comparison between the pure materials is still valid and useful. Finally, we note again that neither Δn nor p influences the form of the color play of the materials, although the twisting power may be modified to place λ_p in the desired wavelength range.

Acknowledgments

The authors thank the SERC for an equipment grant and a studentship in collaboration with BDH Ltd. through the CASE scheme. We also thank BDH Ltd. for provision of the liquid crystal materials and particularly Drs. Ian Sage and Ben Sturgeon for helpful discussions regarding this work.

References

1. H. L. De Vries, *Acta Crystallog.*, **4**, 219 (1951).
2. F. Ania and H. Stegemeyer, *Mol. Cryst. Liq. Cryst. Lett.*, **2**, 67 (1985).
3. H. F. Gleeson and H. J. Coles, submitted to *Liquid Crystals* (1987).
4. J. Constant, D. G. McDonnell and E. P. Raynes, *Mol. Cryst. Liq. Cryst.*, **144**, 161 (1987).
5. G. W. Gray and D. G. McDonnell, *Electron. Lett.*, **11**, 556 (1975); *Mol. Cryst. Liq. Cryst.*, **37**, 189 (1976); *Mol. Cryst. Liq. Cryst.*, **34**, 189 (1976).
6. D. Demus et al., *Z. Chem.*, **17**(2), 64 (1977).
7. BDH Ltd., Poole, Dorset, U.K.

8. H. F. Gleeson, Ph.D. thesis "Optical and Electro-optical Properties of Chiral Mesophases," Manchester, 1986.
9. J. L. Fergason, Proceedings of the 2nd Liquid Crystals Conference, Kent, U.K., Gordon and Breach: NY (1966).
10. E. Merck, D-6100 Darmstadt 1, F.D.R.
11. W. U. Muller and H. Stegemeyer, *Ber. Bunsenges*, **77**, 20 (1973).
12. P. G. De Gennes, *Solid State Comm.*, **10**, 753 (1973).
13. D. McDonnell and I. Sage, "Recent Advances in Medical Thermology" (E. F. Ring and B. Phillips, eds.), Plenum Press (1984), p. 305.
14. J. E. Adams, W. Haas and J. J. Wysocki, in "Liquid Crystals and Ordered Fluids," Plenum, NY (1970), p. 463.
15. H. Stegemeyer and H. Finkelmann, *Chem. Phys. Lett.*, **23**, 227 (1973); *Ber. Bunsenges Phys. Chem.*, **78**, 860 (1974).
16. J. E. Adams and W. Haas, *Mol. Cryst. Liq. Cryst.*, **15**, 27 (1971).
17. P. N. Keating, *Mol. Cryst. Liq. Cryst.*, **8**, 315 (1969).
18. R. A. Alben, *Mol. Cryst. Liq. Cryst.*, **20**, 237 (1973).
19. W. Elser and R. D. Ennulat, Selective Reflection of Cholesteric Liquid Crystals in "Advances in Liquid Crystals" (G. H. Brown, ed.), Academic Press, **2**, 73 (1976).